

Painlevé analysis and integrability of three-dimensional Armbruster Guckenheimer Kim galactic potential

WALID CHATAR¹, JAOUAD KHARBACH¹, MOHAMED BENKHALI¹,
MOHAMED BENMALEK¹, ABDELLAH REZZOUK¹, MOHAMMED
OUAZZANI-JAMIL²

The three-dimensional Armbruster Guckenheimer Kim galactic potential in the general form is considered. The integrability of this problem is performed by using the Painlevé analysis. We report three cases of integrability, exact integrals of motion are obtained explicitly for each case. A numerical experiment is provided to investigate the classical phase space and explore chaos-order-chaos phenomenon.

1. Introduction

Dynamical systems are mathematical notions that can be used to model physical phenomena by differential equations. Using these equations, we can study the evolution over time of dynamical systems and determine their behavior: periodic, quasi-periodic or chaotic. Dynamical systems are used in many branches of physics such as in galactic dynamics.

In general, dynamical systems are described by Hamiltonian mechanics in terms of generalized coordinates q_i and their generalized momenta p_i , these systems are known by Hamiltonian systems. In addition, most of the Hamiltonian systems are not integrable, however, completely integrable systems are very rare in nature and a small perturbation can make them not integrable or chaotic. Even if these systems are very rare, they play a very important role. They allow to test the validity of the fundamental laws of physics.

Galactic dynamics are among the most important branches of astrophysics whose development began during the last seven decades. So, most physicists and astronomers had a vision of the physical world dominated by integrable or quasi-integrable systems (Contopoulos [1]). Many articles have

studied galactic dynamics because this area represents a great challenge for research, these articles have studied several dynamical aspects such as the integrability of a model that can describe the motion of galaxies, for example Armbruster [2], the existence of periodic orbits and their linear stability, see for instance (Llibre and Vidal [3], Alfaro et al. [4], Llibre and Makhlouf [5], Llibre and Roberto [6], Llibre et al. [7]), and the regular and chaotic behaviors of the orbits, see, e.g., (Habib et al. [8], Caranicolas [9], Karanis and Caranicolas [10]). Moreover, chaotic phenomena could play an important role in physical systems and also for galactic dynamics, chaos has taken an important place in the studies that have been made.

Most articles study two types of motion. One of them is studied the global motion in galaxies, as in the axially symmetric mass model that was used by Caranicolas [11]. The other type describes the local galactic motion, and the researches in this type have been centered on the models of elliptic galaxies, because the rotation of these galaxies is made with a low angular velocity (see, e.g., Caranicolas and Barbanis [12], Zeeuw and Merritt [13], Innanen [14]).

To study the integrability of dynamical systems, that is to say the distinction between integrable and non-integrable systems, different methods and approaches exist such as the Painlevé analysis [15, 16], the Ziglin theorem [17], the Liouville theorem [18], Lie algebra [19], separability study [20, 21], the Smaller Alignment index (SALI) method for chaos detection [22], and the Poincaré sections [23].

In general, a physical system whose energy is conserved is modeled by a Hamiltonian system with n degrees of freedom, this Hamiltonian system is integrable in the sense of Liouville, if there exist $n - 1$ other additional integrals in involution $\{H, I_j\} = 0, j = 1, \dots, n - 1$ which are functionally independent [18].

The purpose of this article is to study the integrability of the Hamiltonian with three degrees of freedom, given by:

$$(1.1) \quad H_{3D} = \frac{1}{2}(p_x^2 + p_y^2 + p_z^2) - \frac{\mu}{2}(x^2 + y^2 + z^2) - \frac{\alpha}{4}(x^2 + y^2 + z^2)^2 - \frac{\beta}{2}z^2(x^2 + y^2)$$

where μ, α and β are free arbitrary parameters, p_x, p_y and p_z are generalized momenta corresponding, respectively, to the generalized coordinates x, y and z .

The associated equations of motion are:

$$(1.2) \quad \begin{cases} \dot{p}_x = -\frac{\partial H}{\partial x} = x [\mu + \alpha(x^2 + y^2 + z^2) + \beta z^2], & \dot{x} = \frac{\partial H}{\partial p_x} = p_x \\ \dot{p}_y = -\frac{\partial H}{\partial y} = y [\mu + \alpha(x^2 + y^2 + z^2) + \beta z^2], & \dot{y} = \frac{\partial H}{\partial p_y} = p_y \\ \dot{p}_z = -\frac{\partial H}{\partial z} = z [\mu + (\alpha + \beta)(x^2 + y^2) + \alpha z^2], & \dot{z} = \frac{\partial H}{\partial p_z} = p_z \end{cases}$$

By making use cylindrical coordinates:

$$(1.3) \quad \begin{cases} x = \rho \cos \theta, & p_x = \cos \theta p_\rho - \frac{\sin \theta}{\rho} p_\theta \\ y = \rho \sin \theta, & p_y = \sin \theta p_\rho + \frac{\cos \theta}{\rho} p_\theta \\ z = z, & p_z = p_z \end{cases}$$

The Hamiltonian of the Armbruster-Guckenheimer-Kim becomes

$$(1.4) \quad H_{3D} = \frac{1}{2}(p_\rho^2 + p_z^2) + \frac{k^2}{2\rho^2} - \frac{\mu}{2}(\rho^2 + z^2) - \frac{\alpha}{4}(\rho^2 + z^2)^2 - \frac{\beta}{2}\rho^2 z^2$$

where p_ρ and p_z are generalized momenta corresponding, respectively, to the generalized coordinates ρ and z , while k represents the value of the cyclic integral associated to the cyclic coordinate θ , where $k = p_\theta = xp_y - yp_x$ represents the component of angular momentum about z -axis.

For $k = 0$, H_{3D} is equivalent to a Hamiltonian with two degrees of freedom. This Hamiltonian is known in literature as Hamiltonian of Armbruster-Guckenheimer-Kim (AGK). This potential characterizes the local motion of an almost axisymmetric galaxy that rotates with a constant angular velocity ω around a fixed axis, for this reason (Elmandouh [16]) adds the term ωp_θ which can also appear in several physical problems, but most work has studied the AGK Hamiltonian for $\omega = 0$ (as a non-rotating system), see for instance (Acosta-Humanez [24], Llibre and Roberto [6]).

The first condition for the Hamiltonian of 2D-AGK to be integrable is $\omega = 0$, there are three integrable cases of 2D Hamiltonian: $\beta = 2\alpha$ [16], $\beta = -\alpha$ and $\beta = 0$ [2]. Table 1 shows the Hamiltonian expressions and the second integral of motion for each integrable case.

The article is organized as follows. In Section 2, we studied the integrability of the 3D-AGK problem by using the Painlevé analysis and we compared the results with the 2D-AGK problem. In section 3, we determined the integrables of motion. Numerical investigations are presented in Section 4 to

Table 1: The integrable cases and the corresponding first integrals of motion.

Case	Hamiltonian	Second invariant
$\beta = 0$	$H_{2D} = \frac{1}{2}(p_x^2 + p_y^2) - \frac{\mu}{2}(x^2 + y^2) - \frac{\alpha}{4}(x^2 + y^2)^2$	$I_{2D} = (xp_y - yp_x)^2$
$\beta = -\alpha$	$H_{2D} = \frac{1}{2}(p_x^2 + p_y^2) - \frac{\mu}{2}(x^2 + y^2) - \frac{\alpha}{4}(x^4 + y^4)$	$I_{2D} = p_y^2 - p_x^2 + \mu(x^2 - y^2) + \frac{\alpha}{2}(x^4 - y^4)$
$\beta = 2\alpha$	$H_{2D} = \frac{1}{2}(p_x^2 + p_y^2) - \frac{\mu}{2}(x^2 + y^2) - \frac{\alpha}{4}(x^2 + y^2)^2 - \alpha x^2 y^2$	$I_{2D} = -p_x p_y + \mu xy + \alpha xy(x^2 + y^2)$

confirm the integrability of 3D-AGK and show the transition chaos-order-chaos of this system. Finally, this article is completed by a conclusion that summarizes the obtained results.

2. Painlevé analysis of 3D-AGK

The 3D-AGK is described by the following Hamiltonian:

$$(2.1) \quad H_{3D} = \frac{1}{2}(p_x^2 + p_y^2 + p_z^2) + A(x^2 + y^2 + z^2) + B(x^4 + y^4 + z^4) + Cx^2y^2 + Dz^2(x^2 + y^2)$$

where $A = -\frac{\mu}{2}, B = -\frac{\alpha}{4}, C = -\frac{\alpha}{2}, D = -\frac{(\alpha+\beta)}{2}$

The associated equations of motion are

$$(2.2) \quad \begin{cases} \frac{d^2x}{dt^2} + 2x [A + 2Bx^2 + Cy^2 + Dz^2] = 0 \\ \frac{d^2y}{dt^2} + 2y [A + Cx^2 + 2By^2 + Dz^2] = 0 \\ \frac{d^2z}{dt^2} + 2z [A + D(x^2 + y^2) + 2Bz^2] = 0 \end{cases}$$

The Painlevé analysis contains the following three steps.

2.1. Leading-order behaviors

Considering Eqs.(2.2), we assume that the leading-order behaviors of $x(t), y(t)$ and $z(t)$ in a sufficiently small neighborhood of the movable singularity t_0 are

$$(2.3) \quad x(t) = a_0\tau^p, y(t) = b_0\tau^q, z(t) = c_0\tau^s, \tau = t - t_0 \rightarrow 0$$

and we obtain leading-order equations, by substituting (2.3) in Eqs.(2.2)

$$(2.4) \quad \begin{cases} a_0 p(p-1)\tau^{p-2} + 4Ba_0^3\tau^{3p} + 2Ca_0b_0^2\tau^{p+2q} + 2Da_0c_0^2\tau^{p+2s} = 0 \\ b_0 q(q-1)\tau^{q-2} + 4Bb_0^3\tau^{3q} + 2Ca_0^2b_0\tau^{2p+q} + 2Db_0c_0^2\tau^{q+2s} = 0 \\ c_0 s(s-1)\tau^{s-2} + 4Bc_0^3\tau^{3s} + 2Dc_0(a_0^2\tau^{2p+s} + b_0^2\tau^{2q+s}) = 0 \end{cases}$$

we find from Eqs.(2.4) the following three distinct sets of possibilities

- Case 1: $p = q = s = -1$

$$(2.5) \quad \begin{cases} 2Ba_0^2 + Cb_0^2 + Dc_0^2 = -1 \\ 2Bb_0^2 + Ca_0^2 + Dc_0^2 = -1 \\ 2Bc_0^2 + D(a_0^2 + b_0^2) = -1 \end{cases}$$

- Case 2: $p = s = -1, q = \frac{1}{2} \pm \frac{1}{2} [1 - 8(Ca_0^2 + Dc_0^2)]^{\frac{1}{2}}$

$$(2.6) \quad a_0^2 = c_0^2 = \frac{D - 2B}{4B^2 - D^2}, \quad b_0^2: \text{arbitrary}$$

- Case 3: $p = -1, q = \frac{1}{2} \pm \frac{1}{2} (1 + \frac{4C}{B})^{\frac{1}{2}}, s = \frac{1}{2} \pm \frac{1}{2} (1 + \frac{4D}{B})^{\frac{1}{2}}$

$$(2.7) \quad a_0^2 = -\frac{1}{2B}, \quad b_0^2: \text{arbitrary}, \quad c_0^2: \text{arbitrary}$$

2.2. Resonances

For finding the resonances, we put this form of solutions

$$(2.8) \quad x(t) = a_0\tau^p + \Omega_1\tau^{p+r}, \quad y(t) = b_0\tau^q + \Omega_2\tau^{q+r}, \quad z(t) = c_0\tau^s + \Omega_3\tau^{s+r}$$

we substitute (2.8) into the equations of motion (2.2), and we obtain a system of linear algebraic equations: $M_3(r)\Omega = 0$, $\Omega = (\Omega_1, \Omega_2, \Omega_3)$, where $M_3(r)$ is a 3×3 matrix dependent on r , we calculate $\det M_3(r) = 0$.

For case 1, $p = q = s = -1$

$$(2.9) \quad \det M_3(r) = \begin{vmatrix} r' + 8Ba_0^2 & 4Ca_0b_0 & 4Da_0c_0 \\ 4Ca_0b_0 & r' + 8Bb_0^2 & 4Db_0c_0 \\ 4Da_0c_0 & 4Db_0c_0 & r' + 8Bc_0^2 \end{vmatrix} = 0$$

$$r' = r^2 - 4r$$

It is easy to check that $r' = 4$ is a root of (2.9), and so

$$\begin{aligned}
 (2.10) \quad & (r' - 4)(r' + X)(r' + Y) = 0 \\
 & X + Y = 4 [1 + 2B (a_0^2 + b_0^2 + c_0^2)] \\
 & XY = 4(X + Y) + 16 [(4B^2 - C^2)a_0^2b_0^2 + (4B^2 - D^2)b_0^2c_0^2 + 4(B^2 - D^2)a_0^2c_0^2]
 \end{aligned}$$

From (2.10) we can deduce that the resonances occur at

$$r = -1, 4, \frac{3}{2} \pm \frac{1}{2}(9 - 4X)^{\frac{1}{2}}, \frac{3}{2} \pm \frac{1}{2}(9 - 4Y)^{\frac{1}{2}}$$

The restriction that the resonance values (except -1) be non-negative rationals but must depend on the nature of the leading-order singularity, leads to the following possibilities:

- Case 1(i)

$$(2.11) \quad X = 2, \quad Y = 2, \quad r = -1, 1, 1, 2, 2, 4$$

- Case 1(ii)

$$(2.12) \quad X = 2, \quad Y = 0, \quad r = -1, 0, 1, 2, 3, 4$$

- Case 1(iii)

$$(2.13) \quad X = 0, \quad Y = 0, \quad r = -1, 0, 0, 3, 3, 4$$

For case 2, we obtain the resonance condition after omitting the coefficients of less dominant terms as

$$\det M_3(r) = \begin{vmatrix} r^2 - 3r + 8Ba_0^2 & 0 & 4Da_0c_0 \\ 4Ca_0b_0 & r(r + 2q - 1) & 4Db_0c_0 \\ 4Da_0c_0 & 0 & r^2 - 3r + 8Bc_0^2 \end{vmatrix} = 0$$

which on expanding gives

$$r = -1, 0, 4, (1 - 2q), \frac{1}{2} \left[3 \pm (9 - 4Z)^{\frac{1}{2}} \right] \quad \text{with} \quad Z = 4 [1 + 2B(a_0^2 + c_0^2)]$$

Further, the consideration of non-negative rational resonances in conjunction with the leading-order behaviour leads to the following possibilities:

- Case 2(i)

$$q = 0, Z = 0, \quad Ca_0^2 + Dc_0^2 = 0, B(a_0^2 + c_0^2) = -\frac{1}{2}, \quad r = -1, 0, 0, 1, 3, 4$$

- Case 2(ii)

$$q = 0, Z = 2, \quad Ca_0^2 + Dc_0^2 = 0, B(a_0^2 + c_0^2) = -\frac{1}{4}, \quad r = -1, 0, 1, 1, 2, 4$$

- Case 2(iii)

$$q = -\frac{1}{2}, Z = 0, \quad Ca_0^2 + Dc_0^2 = -\frac{3}{8}, B(a_0^2 + c_0^2) = -\frac{1}{2}, \quad r = -1, 0, 0, 2, 3, 4$$

- Case 2(iv)

$$q = -\frac{1}{2}, Z = 2, \quad Ca_0^2 + Dc_0^2 = -\frac{3}{8}, B(a_0^2 + c_0^2) = -\frac{1}{4}, \quad r = -1, 0, 1, 2, 2, 4$$

For Case 3, in a similar way, we derive the following sets of possibilities:

- Case 3(i)

$$q = 0, \quad s = 0, \quad C = D = 0, \quad r = -1, 0, 0, 1, 1, 4$$

- Case 3(ii)

$$q = 0, \quad s = -\frac{1}{2}, \quad C = 0, \quad D = \frac{3}{4}B, \quad r = -1, 0, 0, 1, 2, 4$$

- Case 3(iii)

$$q = -\frac{1}{2}, \quad s = 0, \quad C = \frac{3}{4}B, \quad D = 0, \quad r = -1, 0, 0, 1, 2, 4$$

- Case 3(iv)

$$q = -\frac{1}{2}, \quad s = -\frac{1}{2}, \quad C = D = \frac{3}{4}B, \quad r = -1, 0, 0, 2, 2, 4$$

2.3. Evaluation of arbitrary constants

Thus we have isolated eleven distinct sets of integer resonances, namely (2.11)–(2.13) for case 1. In order to compute the arbitrary constants for the

above resonances, we introduce the series representations

$$(2.14) \quad x(t) = \sum_{k=0}^4 a_k \tau^{p+k}, y(t) = \sum_{k=0}^4 b_k \tau^{q+k}, z(t) = \sum_{k=0}^4 c_k \tau^{s+k}$$

we substitute (2.13) into the equations of motion (2.2), and for each case, we obtain recursion relations for a_k, b_k and $c_k, k = 0, 1..4$

For case 1, they take the following forms:

$$(2.15) \quad \begin{aligned} (j-1)(j-2)a_j + 2Aa_{j-2} + 4B \sum_l \sum_m a_{j-l-m} a_l a_m + 2C \sum_l \sum_m b_{j-l-m} a_l b_m \\ + 2D \sum_l \sum_m c_{j-l-m} a_l c_m = 0 \end{aligned}$$

$$(2.16) \quad \begin{aligned} (j-1)(j-2)b_j + 2Ab_{j-2} + 4B \sum_l \sum_m b_{j-l-m} b_l b_m + 2C \sum_l \sum_m a_{j-l-m} b_l a_m \\ + 2D \sum_l \sum_m c_{j-l-m} b_l c_m = 0 \end{aligned}$$

$$(2.17) \quad \begin{aligned} (j-1)(j-2)c_j + 2Ac_{j-2} + 4B \sum_l \sum_m c_{j-l-m} c_l c_m + 2D \sum_l \sum_m a_{j-l-m} c_l a_m \\ + 2D \sum_l \sum_m b_{j-l-m} c_l b_m = 0 \end{aligned}$$

where $0 \leq l, m \leq j \leq 4$, by solving (2.15)–(2.17), one can obtain the various a_k, b_k and c_k explicitly.

For example, for $j = 0$

$$\begin{cases} 2Ba_0^2 + Cb_0^2 + Dc_0^2 + 1 = 0 \\ 2Bb_0^2 + Ca_0^2 + Dc_0^2 + 1 = 0 \\ 2Bc_0^2 + D(a_0^2 + b_0^2) + 1 = 0 \end{cases}$$

For $j = 1$

$$\begin{cases} 6Ba_0^2 a_1 + C(2a_0 b_0 b_1 + a_1 b_0^2) + D(2a_0 c_0 c_1 + a_1 c_0^2) = 0 \\ 6Bb_0^2 b_1 + C(2a_0 a_1 b_0 + a_0^2 b_1) + D(2b_0 c_0 c_1 + b_1 c_0^2) = 0 \\ 6Bc_0^2 c_1 + D(a_0^2 c_1 + b_0^2 c_1 + 2a_0 a_1 c_0 + 2b_0 b_1 c_0) = 0 \end{cases}$$

and similarly for $j = 2, 3, 4$, we determine the relations between the constants of the system such as the coefficients a_k, b_k or c_k become arbitrary and we respect the conditions indicated by the resonance values in (2.11)–(2.13). Then, we get the following parametric restrictions:

- Case 1(i): $C = 2B, \quad D = 0, \quad \forall(A, B) \Leftrightarrow \beta = -\alpha, \quad \forall(\mu, \alpha)$

- Case 1(ii): $C = 2B, \quad D = 6B, \quad \forall(A, B) \Leftrightarrow \beta = 2\alpha, \quad \forall(\mu, \alpha)$
- Case 1(iii): $C = D = 2B, \quad \forall(A, B) \Leftrightarrow \beta = 0, \quad \forall(\mu, \alpha)$

Proceeding analogously as before for case 2 we find:

$$\left\{ \begin{array}{l} B = 16B \\ C = D = 12B \\ D = 2B \\ A = 4A \end{array} \right. \quad \text{and} \quad \left\{ \begin{array}{l} B = 8B \\ C = D = 6B \\ D = 2B \\ A = 4A \end{array} \right.$$

For case 3 we find:

$$\left\{ \begin{array}{l} B = 16B \\ C = D = 12B \\ D = 6B \\ A = 4A \end{array} \right. \quad \text{and} \quad \left\{ \begin{array}{l} B = 8B \\ C = 0 \\ D = 0 \\ A = 4A \end{array} \right.$$

Then, these conditions are not logical, and hence, this cases 2 and 3 are omitted.

3. The integrals of motion of 3D-AGK

In this section, we investigate the explicit form of the second and third integrals of motion, in order to substantiate the investigations of the Painlevé analysis of the section 2. For this purpose, let us consider the spherical coordinates (r, θ, φ) , the Hamiltonian (1.1) becomes

$$(3.1) \quad H_{3D} = \frac{1}{2} \left(p_r^2 + \frac{p_\theta^2}{r^2} \right) + \frac{f^2}{2r^2 \sin^2 \theta} - \frac{\mu}{2} r^2 - \frac{\alpha}{4} r^4 - \frac{\beta}{2} r^4 \cos^2 \theta \sin^2 \theta$$

where p_r and p_θ are generalized momenta corresponding, respectively, to the generalized coordinates r and θ , while f represents the value of the cyclic integral associated to the cyclic coordinate φ

$$(3.2) \quad I_1 = p_\varphi = f$$

Moreover, we can determine the cyclic variable φ from $\varphi - \varphi_0 = \int \frac{\delta H}{\delta f} dt$. The Hamilton equations associated with the Hamiltonian (3.1) are given by

$$(3.3) \quad \begin{cases} \dot{p}_r = \frac{p_\theta^2}{r^3} + \frac{f^2}{r^3 \sin^2 \theta} + \mu r + r^3(\alpha + 2\beta \cos^2 \theta \sin^2 \theta), & \dot{r} = p_r \\ \dot{p}_\theta = \frac{f^2 \cos \theta}{r^2 \sin^3 \theta} + \beta r \cos \theta \sin \theta (\cos^2 \theta - \sin^2 \theta), & \dot{\theta} = \frac{p_\theta}{r^2} \end{cases}$$

The integral of energy corresponds to the equations Hamilton (3.3)

$$(3.4) \quad H_{3D} = \frac{1}{2}(p_r^2 + \frac{p_\theta^2}{r^2}) + \frac{f^2}{2r^2 \sin^2 \theta} - \frac{\mu}{2}r^2 - \frac{\alpha}{4}r^4 - \frac{\beta}{2}r^4 \cos^2 \theta \sin^2 \theta = h$$

where h is a constant representing the value of the energy integral.

According to Jacobi’s theory, the Hamilton equations (3.3) are completely integrable, if there exists an integral of the motion I_{3D} independent of the integral of the energy. This integral is known in literatures under the complementary or additional integral name. In general, it is well known that complementary integrals are either quadratic or quartic in terms of momenta. For 3D-AGK, if the complementary integral is quadratic, it takes the form (3.5), but if it is quartic, it takes the form (3.6).

$$(3.5) \quad I_{3D} = I_{2D} + f(\Lambda_3 p_r^2 + \Lambda_2 p_r p_\theta + \Lambda_1 p_\theta^2 + \Lambda_0)$$

$$(3.6) \quad I_{3D} = I_{2D}^2 + f(\Lambda_3 p_r^2 + \Lambda_2 p_r p_\theta + \Lambda_1 p_\theta^2 + \Lambda_0)$$

Where I_{2D} is the complementary integral of 2D-AGK indicated in Table 1 (Using spherical coordinates (r, θ, φ)) and $\Lambda_i (i = 0...3)$ being functions in the generalized coordinates r, θ . Notice that the order of the complementary integral (3.6) is doubled and that we can name doubled order. This situation is found in several problems (see, e.g., Wojciechowski [25], Grammaticos [26]). Note that the quartic integral (3.6) becomes quadratic when $f = 0$.

Using the derivative of I_{3D} with respect to time t or using the Poisson bracket $\{H_{3D}, I_{3D}\}$, by matching the coefficients of moments to zero, using Hamilton equations (3.3), we obtain a system of nonlinear partial differential equations whose solution gives the expressions of $\Lambda_i(r, \theta)$. Thus, the complementary integrals of the three cases are

- Case 1(i) : $\beta = -\alpha$

The complementary integral I_{3D} is quadratic in terms of the momenta

$$(3.7) \quad I_{3D} = I_{2D} + f \left[p_r^2 + \frac{1}{r^2} p_\theta^2 + \frac{f(f-1)}{r^2 \sin^2 \theta} - \mu r^2 - \frac{\alpha}{2} r^4 (1 - 2 \cos^2 \theta \sin^2 \theta) \right]$$

- Case 1(ii) : $\beta = 2\alpha$

The complementary integral I_{3D} is quartic in terms of the momenta

$$(3.8) \quad I_{3D} = I_{2D}^2 + f \left(\frac{f \cos^2 \theta}{r^2 \sin^2 \theta} p_r^2 - \frac{2f \cos \theta}{r^3 \sin \theta} p_r p_\theta + \frac{f}{r^4} p_\theta^2 - 2f \alpha r^2 \cos^2 \theta \right)$$

- Case 1(iii) : $\beta = 0$

The complementary integral I_{3D} is quartic in terms of the momenta

$$(3.9) \quad I_{3D} = \left(p_\theta^2 + \frac{f^2}{\sin^2 \theta} \right)^2$$

It is clear that on a zero level of the cyclic integral $f = p_\varphi = 0$, the complementary integral of each case is reduced to the quadratic integral of 2D-AGK for the same case. In addition, the formula of complementary integrals (3.7), (3.8) and (3.9) are not unique, because any function $Q(I_1, H_{3D})$ can be added to these integrals without its accuracy being affected, because $\dot{Q}(I_1, H_{3D}) = 0$

4. Numerical illustration

Using a set of software routines, to plot 3D trajectories of motion in the phase space for each case, we give numerical illustrations to confirm the three-dimensional integrability of the system. The trajectories of motion are plotted in the phase space (p_y, y, p_x) for cases 1(i) and 1(iii), in the phase space (p_x, z, y) for case 1(ii), we can also choose another phase space to plot the trajectories of motion.

Figures 1, 2 and 3 illustrate the trajectories of motion around case 1(i), we kept two parameters and we varied the third to observe the chaos-order-chaos transition.

In Figure 1, we fixed $\mu = 3$, $\beta = 2$ and we varied α , for $\alpha = -2$ the integrability of the system is satisfied, as it is shown in Figure 1(c), the trajectories of motion are completely regular, if we let us move a little away from the integrable case that is to say for $\alpha = -2.2$ and $\alpha = -1.8$, the system

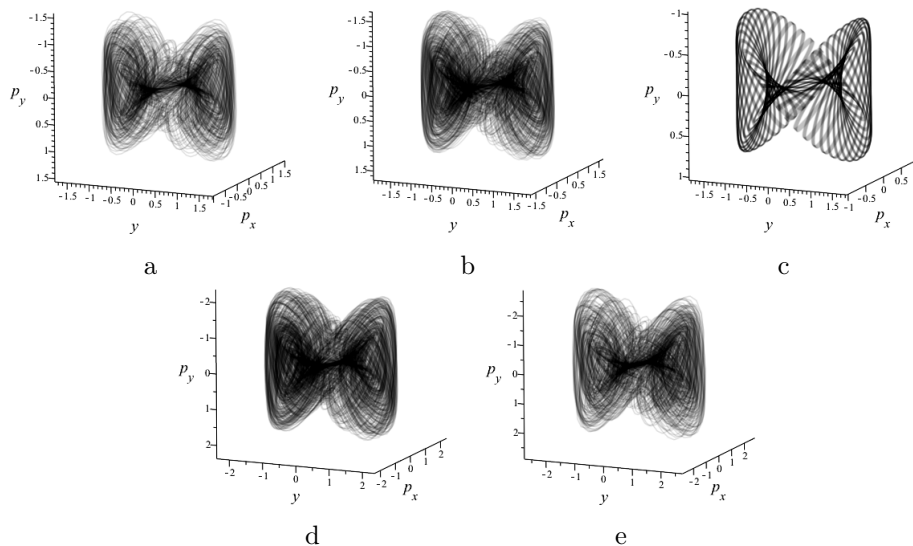


Figure 1: Trajectories of motion in the phase space for case 1(i): $\mu = 3$, $\beta = 2$ and (a) $\alpha = -2.4$, $h = -0.7219$; (b) $\alpha = -2.2$, $h = -0.7429$; (c) $\alpha = -2$, $h = -0.7639$; (d) $\alpha = -1.8$, $h = -0.7849$; (e) $\alpha = -1.6$, $h = -0.8059$

becomes mixed: ordered and chaotic simultaneously, which is clearly visible in Figures 1(b,d), these two values of α present the beginning of chaos when the value of α is varied in both directions $\alpha < -2$ and $\alpha > -2$, when we further increase the value of α in both directions $\alpha = -2.4$ and $\alpha = -1.6$, we observe that the chaotic regions become more dominant than the regular regions which is clearly visible in Figures 1(a,e). In Figure 2, we kept the parameters $\mu = 3$, $\alpha = -2$ and we varied the parameter β in both directions $\beta < 2$ and $\beta > 2$ to observe the chaos-order-chaos transition as it is shown in Figures 2(a-e), since the chaos in the system is most strongly observed in the vicinity of $\beta = 1.75$ and $\beta = 2.5$. In the same way, in Figure 3, we kept the parameters $\alpha = -2$, $\beta = 2$ and we varied the parameter μ , as it is shown in Figures 3(a-e), the chaos-order-chaos phenomenon is not observed because the system is integrable $\forall \mu$ in case 1(i), i.e. the trajectories of motion are completely regular.

Around the case 1(ii), the Figures 4, 5 and 6 illustrate the trajectories of motion for different values of the parameters of the system α , β and μ .

In Figure 4, we fixed the parameters $\mu = 3$, $\beta = -4$ and we varied the parameter α to know the influence of this parameter on the system, for $\alpha =$

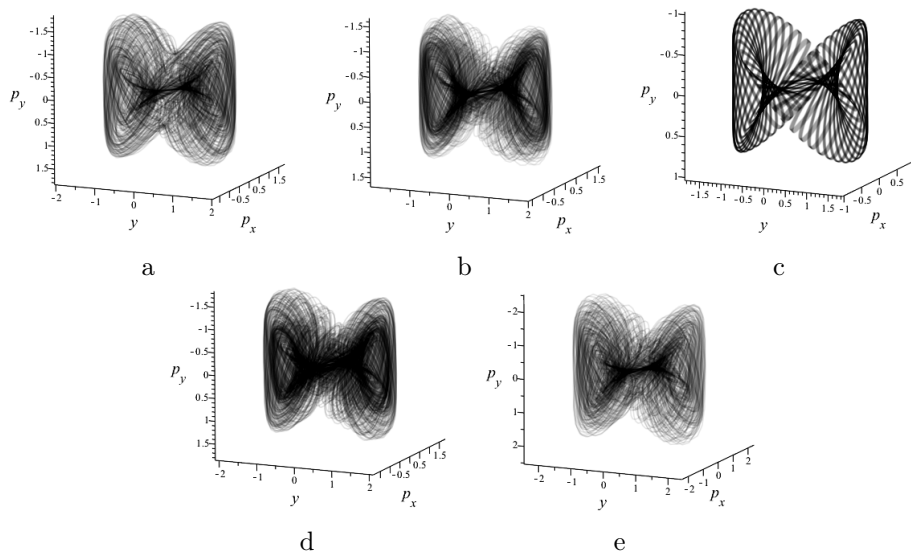


Figure 2: Trajectories of motion in the phase space for case 1(i): $\mu = 3$, $\alpha = -2$ and (a) $\beta = 1.75, h = -0.7633$; (b) $\beta = 1.9, h = -0.7636$; (c) $\beta = 2, h = -0.7639$; (d) $\beta = 2.1, h = -0.7641$; (e) $\beta = 2.5, h = -0.7652$

–2 the system is integrable as it is shown in Figure 4(c), the trajectories of motion are very regular. For $\alpha = -2.2$ and $\alpha = -1.8$ as it is shown in Figures 4(b,d), we observe the beginning of chaos in both directions $\alpha < -2$ and $\alpha > -2$, that is to say, chaotic regions are observed beside regular regions. When the value of α is increased in both directions $\alpha = -2.5$ and $\alpha = -1.5$ as it is shown in Figures 4(a,e), we observe that the chaotic regions which have become more dominant than the regular regions. In Figure 5, we kept the parameters $\mu = 3$, $\alpha = -2$ and varying the parameter β , we observe that the chaos-order-chaos phenomenon is distinctly visible in the trajectories of motion, the system is integrable for $\beta = -4$ as it is shown in Figure 5(c), the system is in the beginning of chaos for $\beta = -4.3$ and $\beta = -3.8$ as it is shown in Figures 5(b,d), we observe more chaotic regions for $\beta = -4.5$ and $\beta = -3.5$ as it is shown in Figures 5(a,e). If we vary the parameter μ , the system is always integrable as it is shown in Figures 6(a-e).

In the same way as the two cases above, we kept two parameters and we varied the third, to show the influence of each parameter on the integrability of the system. Figures 7, 8 and 9 illustrate the trajectories of motion around case 1(iii) for different values of the parameters of the system α , β and μ .

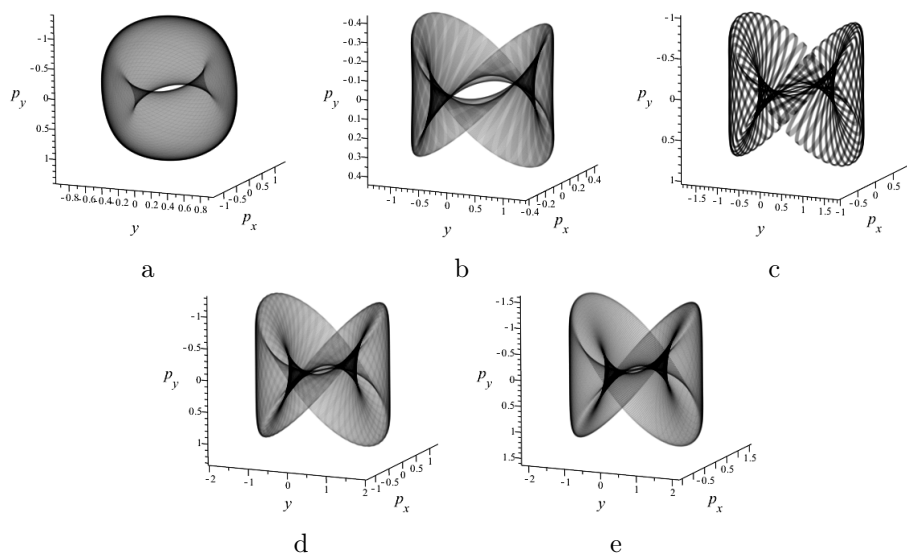


Figure 3: Trajectories of motion in the phase space for case 1(i): $\alpha = -2$, $\beta = 2$ and (a) $\mu = -1.5, h = 0.6939$; (b) $\mu = 2, h = -0.4399$; (c) $\mu = 3, h = -0.7639$; (d) $\mu = 3.5, h = -0.9259$; (e) $\mu = 4, h = -1.0879$

The system is always integrable when we varied the parameters α and μ because the condition of integrability in case 1(iii) is $\beta = 0$, that is to say does not depend on the parameters α and μ , so the chaos-order-chaos phenomenon is not observed. To confirm this result we varied these parameters, as it is shown in Figures 7(a-e) for α and Figures 9(a-e) for μ . The chaos-order-chaos transition is shown in Figure 8 when we varied the parameter β . For $\beta = 0$ as it is shown in Figure 8(c), the integrability of the system is satisfied, for $\beta = -0.5$ and $\beta = 0.4$ as it is shown in Figures 8(b,d) we have the beginning of chaos, and we observe chaotic regions in the vicinity of regular regions, the chaotic behavior increases when $\beta = -1$ and $\beta = 0.7$ as it is shown in Figures 8(a,e).

According to the Figures 1-9 that represent the trajectories of motion around the three integrable cases of the system, when the parameters α , β and μ are varied, we show that chaos-order-chaos transition is a robust phenomenon, i.e. the mechanism of the transition changes rapidly if one of the parameters of the system is varied, except for the parameter μ and the parameter α for case 1 (iii). We deduce that the parameter μ does not change the integrability of the system for the three cases. For the variation of the

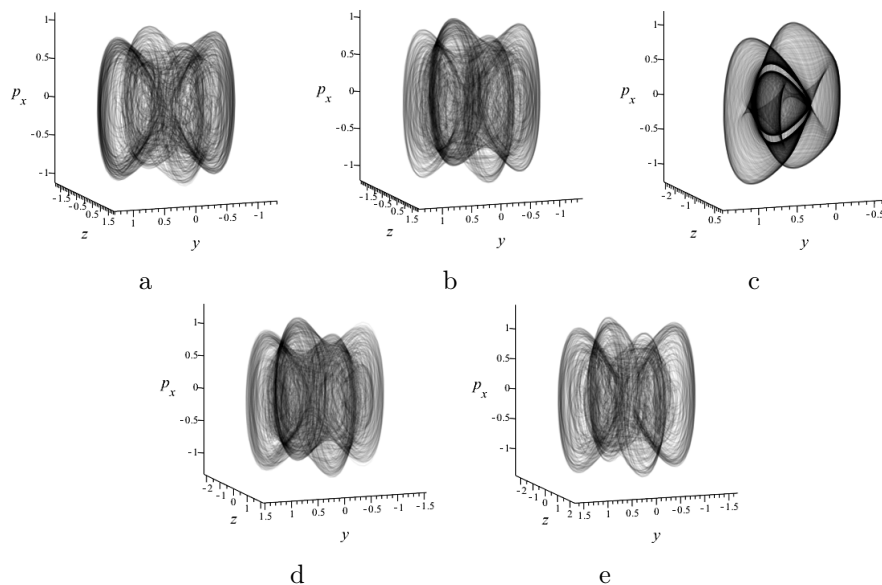


Figure 4: Trajectories of motion in the phase space for case 1(ii): $\mu = 3$, $\beta = -4$ and (a) $\alpha = -2.5, h = -0.2297$; (b) $\alpha = -2.2, h = -0.2306$; (c) $\alpha = -2, h = -0.2311$; (d) $\alpha = -1.8, h = -0.2317$; (e) $\alpha = -1.5, h = -0.2326$

parameter α , the behavior of the system is changed in the vicinity of the integrable cases except for case 1(iii), the variation of parameter β shows the chaos-order-chaos transition for the three integrable cases of the system, i.e. a small perturbation allows to change the behavior of system.

5. Conclusion

To conclude, we have studied the integrability of 3-dimensional Armbruster-Guckenheimer-Kim Hamiltonian 3D-AGK, for this reason we determined the integrable cases by using the Painlevé analysis and we found three cases as in the 2D-AGK. In order to confirm integrability of the 3D-AGK, we have accompanied this analysis by the construction of the additional first integrals of motion for each case. Only in this way, the powerful predictive nature of the method will be materialized. However, the possibility of existence of other integrable cases far from the known ones should not be ruled out until the contrary is proven.

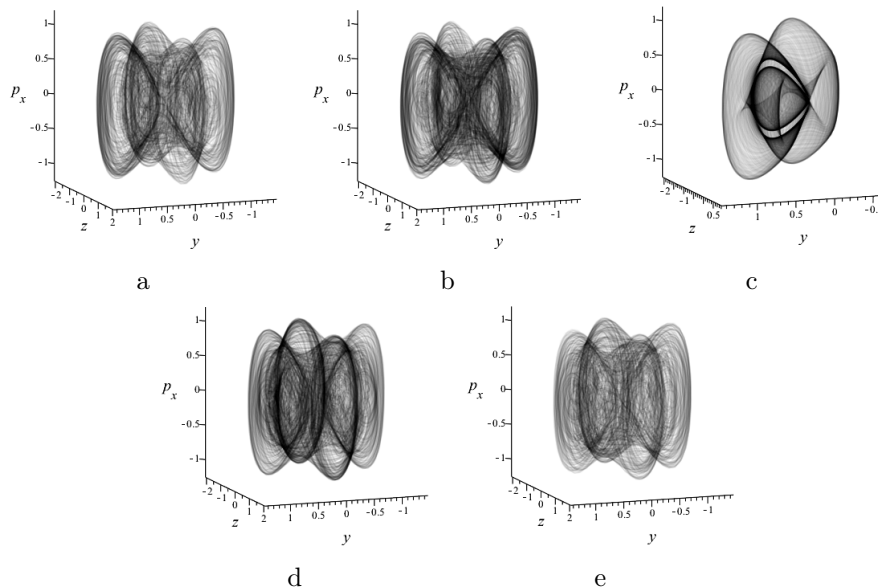


Figure 5: Trajectories of motion in the phase space for case 1(ii): $\mu = 3$, $\alpha = -2$ and (a) $\beta = -4.5, h = -0.23115$; (b) $\beta = -4.3, h = -0.23117$; (c) $\beta = -4, h = -0.23119$; (d) $\beta = -3.8, h = -0.23120$; (e) $\beta = -3.5, h = -0.23122$

Finally, we have explored the chaos-order-chaos phenomenon in detail by working with the variation of the system control parameters. We deduce that the parameter μ does not change the integrability of the system for the three cases, but the system is very sensitive to the variation of the parameter β for the three cases and admits a strong sensitivity for the parameters α in cases 1(i) and 1(ii), but the variation of α does not influence the system in case 1(iii).

References

- [1] G. Contopoulos, N. Voglis and C. Kalapotharakos, *Order and chaos in self-consistent galactic models*. Modern Celestial Mechanics: From Theory to Application., 191-204, (2002).
- [2] D. Armbruster, J. Guckenheimer and S. Kim, *Chaotic dynamics in systems with square symmetry*. Phys. Lett. A., **140**, 416-420, (1989).

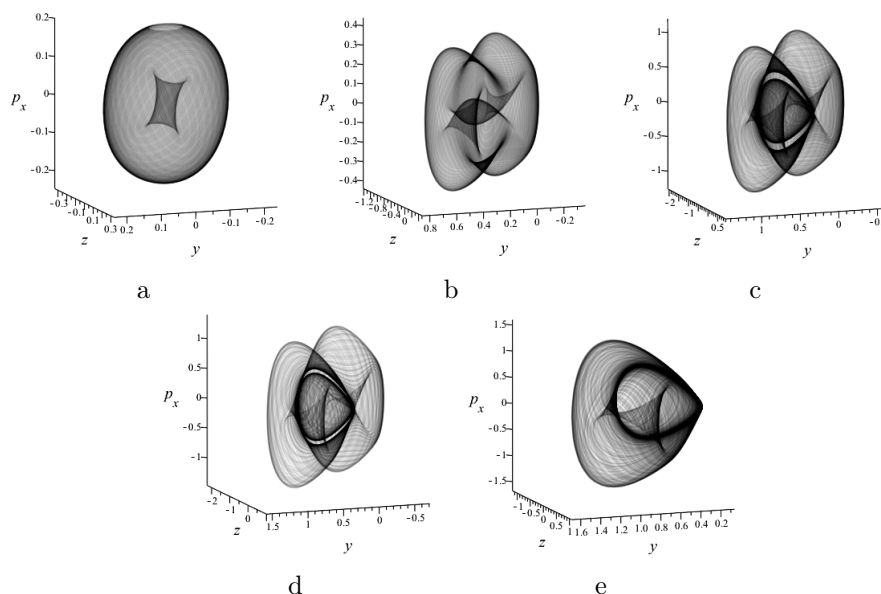


Figure 6: Trajectories of motion in the phase space for case 1(ii): $\alpha = -2$, $\beta = -4$ and (a) $\mu = -1, h = 0.4528$; (b) $\mu = 1, h = 0.1108$; (c) $\mu = 3, h = -0.2311$; (d) $\mu = 3.5, h = -0.3166$; (e) $\mu = 4, h = -0.4021$

- [3] J. Llibre and C. Vidal, *Periodic orbits and non-integrability in a cosmological scalar field*. J. Math. Phys., **53**, 12702, (2012).
- [4] F. Alfaro, J. Llibre and E. Pérez-Chavela, *Periodic orbits for a class of galactic potentials*. Astrophys. Space Sci., **344**, 39-44, (2013).
- [5] J. Llibre and A. Makhlouf, *Periodic orbits of the generalized Friedmann-Robertson-Walker Hamiltonian systems*. Astrophys. Space Sci., **344**, 45-50, (2013).
- [6] J. Llibre and L. Roberto, *Periodic orbits and non-integrability of Armbruster-Guckenheimer-kim potential*. Astrophys. Space Sci., **343**, 69-74, (2013).
- [7] J. Llibre, D. Pasca and C. Valls, *Periodic solutions of a galactic potential*. Chais, Solitons and Fractals., **61**, 38-43, (2014).
- [8] S. Habib, H.E. Kandrup and M.E. Mahon, *Chaos and noise in galactic potentials*. Astrophys. J., **480**, 155, (1997).

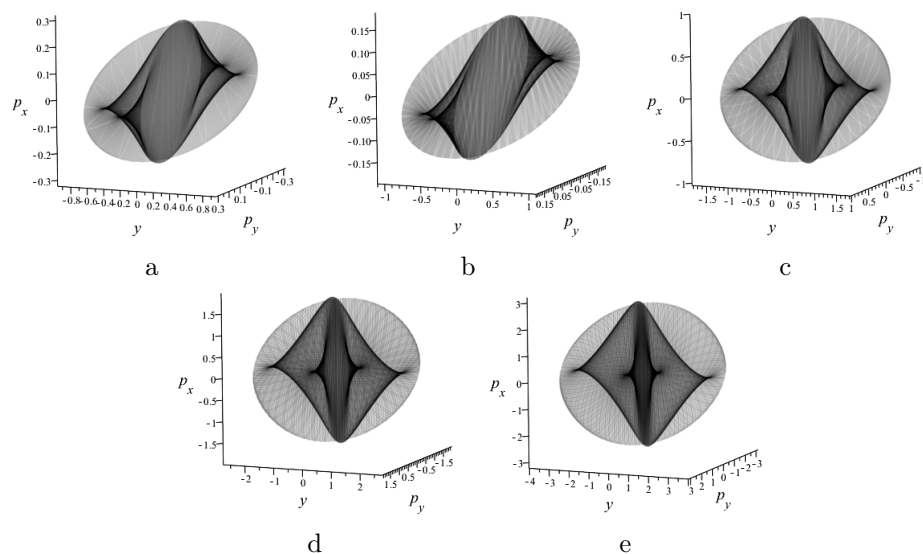


Figure 7: Trajectories of motion in the phase space for case 1(iii): $\mu = 3$, $\beta = 0$ and (a) $\alpha = -6, h = -0.3390$; (b) $\alpha = -4, h = -0.5489$; (c) $\alpha = -2, h = -0.7588$; (d) $\alpha = -1, h = -0.8638$; (e) $\alpha = -0.5, h = -0.9162$

- [9] N.D. Caranicolas, *Maps describing motion in strong bars*. *New Astron.*, **5**, 397-402, (2000).
- [10] G.I. Karanis and N.D. Caranicolas, *Transition from regular motion to chaos in a logarithmic potential*. *Astron. Astrophys.*, **367**, 443-448, (2001).
- [11] N.D. Caranicolas, *The structure of motion in a 4-component galaxy mass model*. *Astrophys. Space Sci.*, **246**, 15-28, (1996).
- [12] N.D. Caranicolas and B. Barbanis, *Periodic orbits in nearly axisymmetric stellar systems*. *Astron. Astrophys.*, **114**, 360-366, (1982).
- [13] P.T. De Zeeuw and D. Merritt, *Stellar orbits in a triaxial galaxy. I-Orbits in the plane of rotation*. *Astrophys. J.*, **267**, 571, (1983).
- [14] K.A. Innanen, *The threshold of chaos for Henon-Heiles and related potentials*. *Astron. J.*, **90**, 2377-2380, (1985).
- [15] W. Chatar, M. Benkhali, I. El Fakkousy, J. Kharbach, A. Rezzouk and M. Ouazzani-Jamil, *The hydrogen atom in the van der Waals potential*

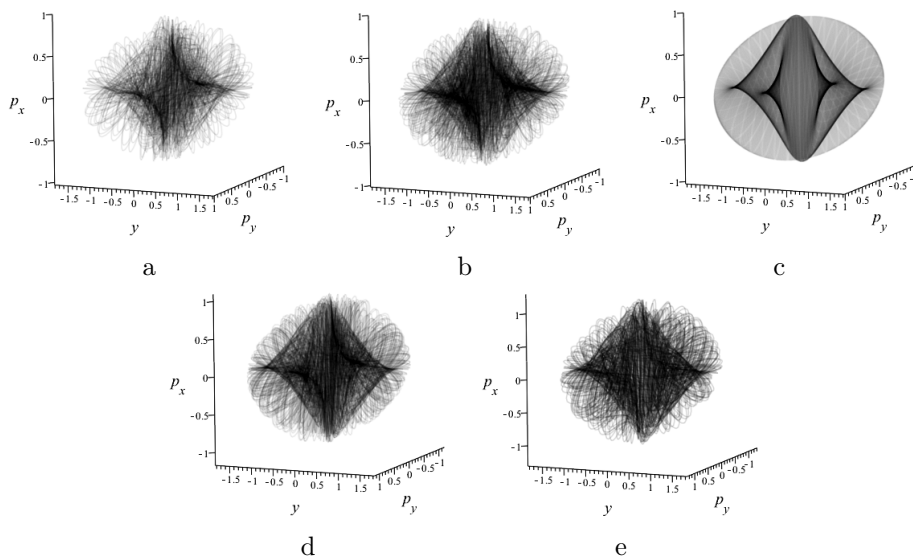


Figure 8: Trajectories of motion in the phase space for case 1(iii): $\mu = 3$, $\alpha = -2$ and (a) $\beta = -1, h = -0.7563$; (b) $\beta = -0.5, h = -0.7575$; (c) $\beta = 0, h = -0.7588$, (d) $\beta = 0.4, h = -0.7598$; (e) $\beta = 0.7, h = -0.7606$

combined by magnetic and electric fields, Painlevé analysis, and integrability. J. Math. Phys, **60**, 62702, (2019).

[16] A.A. Elmandouh, *On the dynamics of Armbruster Guckenheimer kim galactic potential in a rotating reference frame.* Astrophys. Space Sci., **361**, 182, (2016).

[17] J.J. Morales and C. Simó, *Picard-Vessiot Theory and Ziglin’s Theorem.* J. Differ. Equ., **107**, 140-162, (1994).

[18] R. Abraham and J.E. Marsden, *Foundation of mechanics.* Benjamin/Cummings Publishing Company Reading, Massachusetts, **36**, (1978).

[19] R.Z. Zhdanov, *Lie symmetry and integrability of ordinary differential equations.* J. Math. Phys., **39**, 6745-6756, (1998).

[20] W. Chatar, M. Benkhali, I. El Fakkousy, J. Kharbach, A. Rezzouk and M. Ouazzani-Jamil, *Classical mechanics of the Hydrogen atom perturbed*

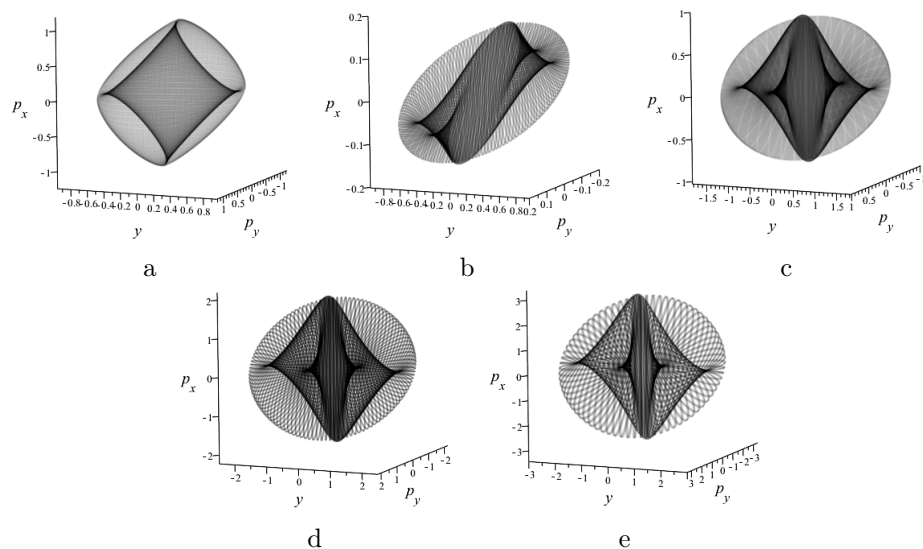


Figure 9: Trajectories of motion in the phase space for case 1(iii): $\alpha = -2$, $\beta = 0$ and (a) $\mu = -1, h = 0.5370$; (b) $\mu = 1, h = -0.1109$; (c) $\mu = 3, h = -0.7588$; (d) $\mu = 5, h = -1.4068$; (e) $\mu = 7, h = -2.0547$

by Van der Waals potential interacting with combined electric and magnetic fields. *Journal of Physics: Conference Series*, **1292**, 12008, (2019).

- [21] W. Chatar, M. Benkhali, I. El Fakkousy, J. Kharbach, A. Rezzouk and M. Ouazzani-Jamil, *The phase topology and bifurcation tori of the Hydrogen atom subjected to external fields*. *Journal of Physics: Conference Series*, **1292**, 12007, (2019).
- [22] L.A. Caritá, I. Rodrigues, I. Puerari and L.E.C.A. Schiavo, *Using the SALI method to distinguish chaotic and regular orbits in barred galaxies with the LP-VIcode program*. *Prog. Phys.*, **13**, 161, (2017).
- [23] C.L. Goudas, K.E. Papadakis and G.A. Katsiaris, *Numerical investigation of the galactic problem by computing families of periodic solutions*. *Astrophys. Space Sci.*, **301**, 97-116, (2006).
- [24] P. Acosta-Humánez, M. Alvarez-Ramírez and T.J. Stuchi, *Nonintegrability of the Armbruster–Guckenheimer–kim Quartic Hamiltonian Through Morales–Ramis Theory*. *SIAM J. Appl. Dyn. Syst.*, **17**, 78-96, (2018).

- [25] S. Wojciechowski, *Integrability of one particule in a perturbed central quartic potential*. Phys. Scr., **31**, 433, (1985).
- [26] B. Grammaticos, B. Dorizzi, A. Ramani and J. Hietarinta, *Extending integrable Hamiltonian systems from 2 to N dimensions*. Phys. Lett. A., **109**, 81-4, (1985).

¹LABORATOIRE DE PHYSIQUE DU SOLIDE, FACULTÉ DES SCIENCES DHAR EL MAHRAZ, UNIVERSITÉ SIDI MOHAMED BEN ABDELLAH, B.P. 1796, 30000 FEZ-ATLAS, MOROCCO.

²LABORATOIRE SYSTÈMES ET ENVIRONNEMENTS DURABLES, UNIVERSITÉ PRIVÉE DE FÈS, LOT. QUARAOUYINE ROUTE AIN CHKEF, 30040 FEZ, MOROCCO.

E-mail address: walid.chatrar@usmba.ac.ma

